Control of hysteresis: theory and experimental results*

Xiaobo Tan[†], Ram Venkataraman[‡], and P. S. Krishnaprasad[†]

[†]Institute for Systems Research and
Department of Electrical and Computer Engineering
University of Maryland, College Park, MD 20742 USA
[‡]Veridian Engineering and
Wright-Patterson AFB, OH 45433-7531 USA

ABSTRACT

Hysteresis in smart materials hinders the wider applicability of such materials in actuators. In this paper, a systematic approach for coping with hysteresis is presented. The method is illustrated through the example of controlling a commercially available magnetostrictive actuator.

We utilize the low-dimensional model for the magnetostrictive actuator that was developed in earlier work. For low frequency inputs, the model approximates to a rate-independent hysteresis operator, with current as its input; magnetization as its output. Magnetostrictive strain is proportional to the square of the magnetization. In this paper, we use a classical Preisach operator for the rate-independent hysteresis operator.

In this paper, we present the results of experiments conducted on commercial magnetostrictive actuators, the purpose of which was the control of the displacement/strain output. A constrained least-squares algorithm is employed to identify a discrete approximation to the Preisach measure. We then discuss a nonlinear inversion algorithm for the resulting Preisach operator, based on the theory of strictly-increasing operators. This algorithm yields a control input signal to produce a desired magnetostrictive response. The effectiveness of the inversion scheme is demonstrated via an open-loop trajectory tracking experiment.

Keywords: Control, hysteresis, Preisach, identification, inversion, magnetostriction, smart actuator

1. INTRODUCTION

Hysteresis in smart materials, e.g., magnetostrictives, piezoceramics, and Shape Memory Alloys (SMAs), hinders the wider applicability of such materials in actuators. A fundamental idea in coping with hysteresis is to formulate the mathematical model of hysteresis and use inverse compensation to cancel out the hysteretic effect. This idea can be found in the works of Tao and Kokotović,[1] Smith,[2] and Galinaitis and Rogers,[3] to name a few.

Hysteresis models for smart materials can be classified into physics based models and phenomenological models. An example of physics based model is the Jiles-Atherton model for ferromagnetic hysteresis,[4] where hysteresis is considered to arise from pinning of domain walls on defect sites. The most popular phenomenological hysteresis model used in control of smart actuators has been the Preisach model.[5–7] A similar type of operator, called Krasnoselskii-Pokrovskii (KP) operator was used by Galinaitis and Rogers in modeling a piezoelectric actuator.[3] Though the Preisach model does not provide any physical insight into the problem, it provides a means of developing phenomenological models that are capable of producing behaviors similar to physical systems(see Mayergoyz[8] for an excellent exposition).

In this paper we present a systematic approach for control of smart actuators. The method is illustrated through the example of controlling a commercially available magnetostrictive actuator. The model we use for the magnetostrictive actuator is based on earlier work of our group.[13,?] It was shown that a key component of a low-order model is as shown in Figure 4. The rate-independent hysteresis operator is a classical Preisach operator followed by a squaring operator. The input of the hysteresis operator is the current input to the actuator, and the output of the squaring operator is a quantity with the dimensions of force. In this paper, we deal with low frequency inputs

* This research was supported by the Army Research Office under the ODDR&E MURI97 Program Grant No. DAAG55-97-1-0114 to the Center for Dynamics and Control of Smart Structures (through Harvard University).
Further author information: (Send correspondence to X.T.)
E-mail: X.T.: xbtan@isr.umd.edu R.V.: ram.venkataraman@wpafb.af.mil P.S.K.: krishna@isr.umd.edu

of less than 5 Hz, as we wish to focus on the hysteresis operator only. For this case, the linear system in Figure 4 approximates to a constant with dimensions of length/force.

A constrained least-squares algorithm is employed to identify a discrete approximation to the Preisach measure (also called weighting function in literature). We then discuss a nonlinear inversion algorithm for the resulting Preisach operator, based on the theory of strictly-increasing operators. This algorithm yields a control input signal to produce a desired magnetostrictive response.

The remainder of the paper is organized as follows. Section 2 provides an introduction to the Preisach operator, where the emphasis is put on how to evaluate the output of the Preisach operator given an initial memory curve and the input. Disretization scheme and identification algorithm will be discussed in Section 3. Section 4 is devoted to an inverse algorithm, which fully exploits the strictly-increasing property of the Preisach operator and the discrete structure of the problem. Experimental results are given in Section 5. Concluding remarks and discussions on possible future work are provided in Section 6.

2. THE PREISACH MODEL

Consider a simple hysteretic element (relay) shown in Figure 1. The relationship between the "input" variable u and the "output" variable v at each instant of time t can be described by:

$$\begin{cases} v = +1 \quad \text{if} \quad u > \alpha, \\ v = -1 \quad \text{if} \quad u < \beta, \\ v \quad \text{remains unchanged if} \quad \beta \leq u \leq \alpha. \end{cases} \qquad (1)$$

Call the operator relating $u(\cdot)$ to $v(\cdot)$ as $\hat{\gamma}_{\beta,\alpha}[u](\cdot)$, where we now view the input and output variables as functions of time. This operator is sometimes referred to as an *elementary Preisach hysteron* since it is a basic block from which the Preisach operator $\Gamma[\cdot]$ will be constructed. We now outline this construction. Suppose $u(\cdot) \in C[0,T]$ is the input to the elementary hysteron. The output of the Preisach operator is defined as:

$$\omega(t) = \Gamma[u](t) = \int\int_{\alpha \geq \beta} \mu(\beta,\alpha)\hat{\gamma}_{\beta,\alpha}[u](t) d\beta d\alpha, \qquad (2)$$

where $\mu(\cdot,\cdot)$ is a *density function (*also called *weighting function* or the *Preisach measure).* This representation is the most natural one for the Preisach operator and is closest to Preisach's original definition.[8] The Preisach operator has *non-local* memory and it "remembers" the dominant maximum and minimum values of the past input. For a review of this and other basic properties of the Preisach operator, please refer to Mayergoyz[8] and Brokate and Sprekels.[10]

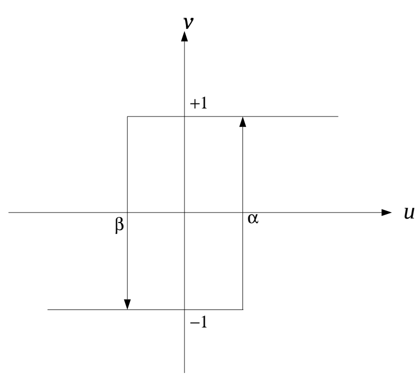

Figure 1.
Illustration of the Elementary Preisach Hysteron

The memory effect of the Preisach operator can be captured by curves in the *Preisach* (β,α) *plane.* To simplify the discussion, we assume the Preisach measure $\mu(\cdot,\cdot)$ has a compact support, i.e., $\mu(\beta,\alpha) = 0$ if $\beta < \beta_0$ or $\alpha > \alpha_0$

for some β_0, α_0. Then the Preisach plane $P \stackrel{\triangle}{=} \{(\beta, \alpha) | \alpha \geq \beta, \beta \geq \beta_0, \alpha \leq \alpha_0\}$. Each $(\beta, \alpha) \in P$ is identified with the hysteron $\hat{\gamma}_{\beta,\alpha}$, as shown in Figure 2(a). At each time instant t, P can be divided into two regions:

$$P\_(t) \stackrel{\triangle}{=} \{(\beta, \alpha) \in P| \quad \text{output of } \hat{\gamma}_{\beta,\alpha} \text{ at } t \text{ is} -1\},$$
$$P_+(t) \stackrel{\triangle}{=} \{(\beta, \alpha) \in P| \quad \text{output of } \hat{\gamma}_{\beta,\alpha} \text{ at } t \text{ is} +1\},$$

so that $P = P\_(t) \cup P_+(t)$ at all times. Equation (2) can be rewritten as:

$$\omega(t) = \int\int_{P_+(t)} \mu(\beta, \alpha) d\beta d\alpha - \int\int_{P\_(t)} \mu(\beta, \alpha) d\beta d\alpha. \tag{3}$$

Now assume that at some initial time t_0, the input $u(t_0) = u_0 < \beta_0$. Then the output of every hysteron operator is -1. Therefore $P\_(t_0) = P$, $P_+(t_0) = \emptyset$ and it corresponds to the "negative saturation"(Figure 2(b)). Next we assume that the input is monotonically increased to some maximum value at t_1 with $u(t_1) = u_1$. The output of $\hat{\gamma}_{\beta,\alpha}$ is switched to +1 as the input $u(t)$ increases past α. Thus at time t_1, the boundary between $P\_(t_1)$ and $P_+(t_1)$ is the horizontal line $\alpha = u_1$(Figure 2(c)). Next we assume that the input starts to decrease monotonically until it stops at t_2 with $u(t_2) = u_2$. It's easy to see that the output of $\hat{\gamma}_{\beta,\alpha}$ becomes -1 as $u(t)$ sweeps past β, and correspondingly, a vertical line segment $\beta = u_2$ is generated as part of the boundary(Figure 2(d)). Further input reversals generate additional horizontal or vertical boundary segments.

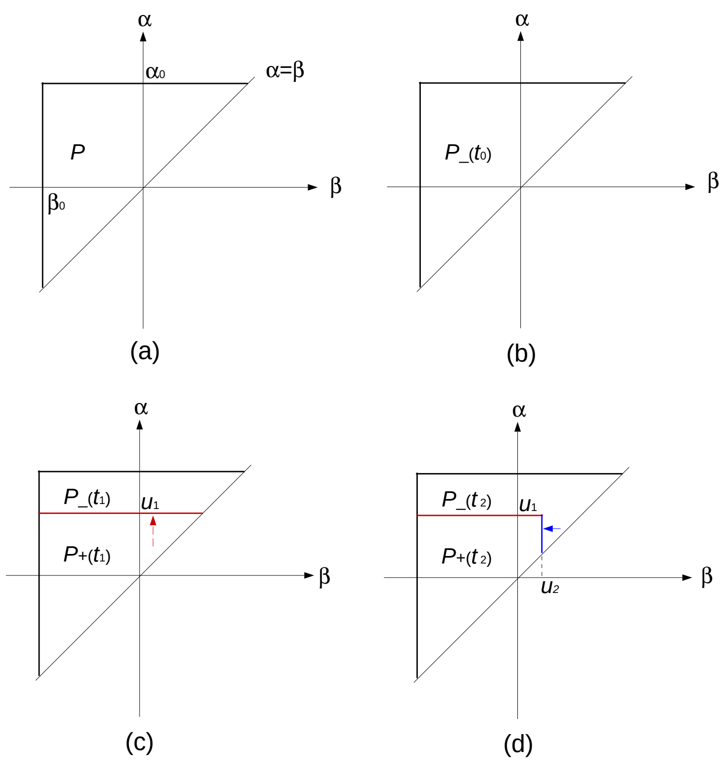

Figure 2.

Memory Curve in the Preisach Plane

From the above illustration, we can see that each of $P\_$ and P_+ is a connected set, and the output of the Preisach operator is determined by the boundary between $P\_$ and P_+. The boundary is also called *memory curve*, since it provides information about the state of any hysteron. We also note that due to its staircase structure, the memory curve is fully captured by its corner points, which correspond exactly to the past dominant maximum and minimum input values. Motivated by this observation, we store and update only these corner points in our numerical implementation of the Preisach model.

3. IDENTIFICATION OF THE PREISACH MEASURE

3.1. Review of identification methods

A classical method for identifying the Preisach measure is using the so called *first order reversal curves*, detailed in Mayergoyz.[8] A first order reversal curve can be generated by first bringing the input to the negative saturation, followed by a monotonic increase to α, then a monotonic decrease to β. The term "first order reversal" comes from the fact that each of these curves is formed after the first reversal of the input. Denote the output value as $f(\beta, \alpha)$ when the input reaches β. Then the measure $\mu(\beta, \alpha)$ can be obtained as

$$\mu(\beta, \alpha) = \frac{1}{2} \frac{\partial^2 f(\beta, \alpha)}{\partial \beta \partial \alpha}. \tag{4}$$

Equatin (4) is useful only when the two-dimensional surface $f(\beta, \alpha)$ is smooth, which is not the case for measured curves in experiments. To overcome this difficulty, a smooth approximation surface $\tilde{f}(\beta, \alpha)$ is fit to the data points.[6,7] Hughes and Wen[6] approximated the surface by polynomials using a least squares method. Gorbet, Wang and Morris employed functions with specific forms, and the parameters were obtained via a weighted least square algorithm.[7] As pointed out in Gorbet, Wang and Morris,[7] deriving the measure by differentiating a fitted surface is inherently imprecise, since different type of approximating functions lead to quite different measure distributions.

Hoffmann and Sprekels[11] proposed a scheme to identify the Preisach measure directly. By devising the input sequence carefully, they set up independent blocks of linear equations involving the output measurements and the atomic measures in the discretized Preisach plane. Each block of equations can be solved successively to obtain the measures. This scheme is very sensitive to experimental errors as one can easily see. Using the identified discrete measures,[11] Hoffman and Meyer[12] approximated the (continuous) Preisach measure in terms of a set of basis functions. A least squares method was applied to compute the coefficients.

Another way to obtain the measure is driving the system with a "reasonably" rich input signal, measuring the output and then estimating the Preisach measure by a least squares method. Galinaitis and Rogers[3] used this idea to identify the weights for a KP operator. We will also adopt this method for measure identificaiton in this paper.

3.2. Identification scheme

Magnetostrictive actuators, due to the capacity of the windings or other practical reasons, have to be operated with their inputs within a specific range. As a consequence, we will not be able to visit the whole Preisach plane and identify the measure everywhere during the identification process. We assume the input range is $[u_{min}, u_{max}]$. Since the input $u(t)$ never goes beyond the limits, the state of hysterons in the area Ω_0 (Figure 3) remain unchanged. Thus the bulk contribution to the output from Ω_0 is a constant and we denote it by ω_0.

The input is discretized into L levels uniformly and we label the discretized Preisach plane as illustrated in Figure 3. The quantities we want to identify include atom measures $\mu_{ij}, i = 1, \cdots, L, j = 1, \cdots, i$ and ω_0. To simplify the discussion, with a little bit notation abuse, we write $\mu_{ij}, i = 1, \cdots, L, j = 1, \cdots, i$ into a column vector $\mu_k, k = 1, \cdots, K$, where $K = \frac{L(L+1)}{2}$.

To initialize the states of hysterons, We first increase the input to u_{max} and then reduce it to u_{min}. This sets the state of each hysteron in P/Ω_0 to -1. We may also initialize each hysteron to +1 by decreasing the input to u_{min} followed by bringing it to u_{max}. We then apply some piecewise monotone continuous input $u(t), t \in [0, T]$ which contains sufficient information, and measure the output $\omega(t)$. Signal $u(t), \omega(t)$ are sampled into sequences $u[n], \omega[n], n = 1, \cdots, N$. The input sequence $u[n]$ (after discretization) is fed into the discretized Preisach operator and the state of each hysteron, $\hat{\gamma}_k[n], k = 1, \cdots, K$ is computed. The output of the Preisach model at time instant n can be expressed as:

$$\tilde{\omega}[n] = \omega_0 + \sum_{k=1}^{K} \mu_k \hat{\gamma}_k[n], \tag{5}$$

where $\mu_k's$ are yet to be found.

We use the least squares method to estimate the parameters, i.e. the parameters are determined in such a way that

$$\sum_{n=1}^{N} |\omega[n] - \tilde{\omega}[n]|^2 \tag{6}$$

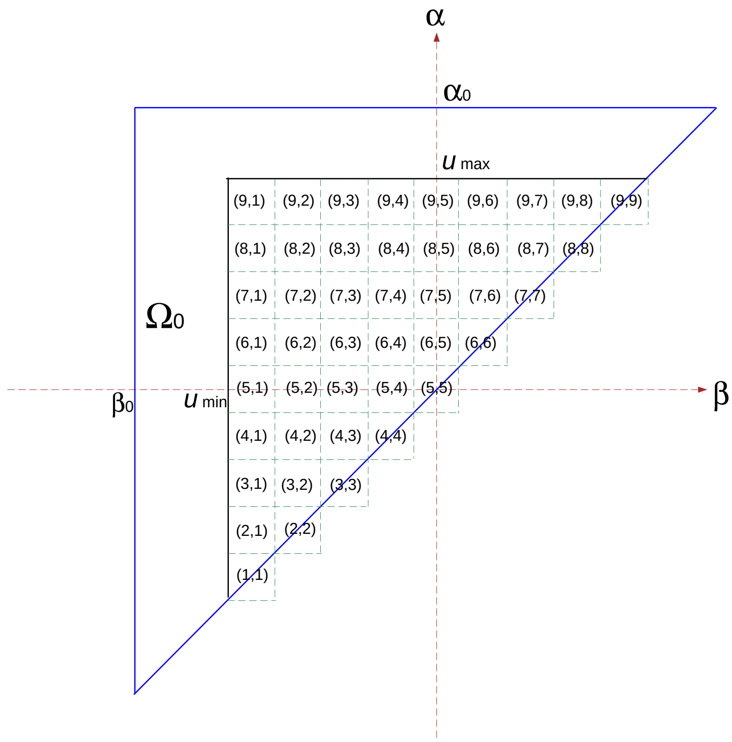

Figure 3.

Discretization of the Preisach plane ($L = 9$)

is minimized. This can be written in a more compact form. Let

$$\theta = \begin{bmatrix} \mu_1 \\ \mu_2 \\ \vdots \\ \mu_K \\ \omega_0 \end{bmatrix}, \quad A = \begin{bmatrix} \hat{\gamma}_1[1] & \hat{\gamma}_2[1] & \cdots & \hat{\gamma}_K[1] & 1 \\ \hat{\gamma}_1[2] & \hat{\gamma}_2[2] & \cdots & \hat{\gamma}_K[2] & 1 \\ \vdots & \vdots & \vdots & \vdots & \vdots \\ \hat{\gamma}_1[N] & \hat{\gamma}_2[N] & \cdots & \hat{\gamma}_K[N] & 1 \end{bmatrix}, \quad b = \begin{bmatrix} \omega[1] \\ \omega[2] \\ \vdots \\ \omega[N] \end{bmatrix}.$$

Then the problem becomes finding the parameter vector θ, such that

$$\| A\theta - b \|$$

is minimized, where $\| \cdot \|$ stands for the Euclidean norm in R^N. Since we require $\mu_k \geq 0, k = 1, \cdots, K$, it is a least square error optimization problem with constraints.

4. INVERSION OF THE PREISACH OPERATOR

The general structure of models for smart actuators that capture both hysteresis and dynamic behaviour is shown in Figure 4. In the figure, $G(s)$ represents the transfer function of the linear part in the actuator, while W denotes a rate-independent hysteretic nonlinearity. Venkataraman[13] has shown that a key component of a low-order model for magnetostriction in Terfenol-D has a structure resembling Figure 4.

A basic idea for controller synthesis for such systems is to design an right inverse operator W^{-1} for W as shown in Figure 5. Then $\omega(\cdot) = \bar{u}(\cdot)$ and the controller design problem is reduced to designing a linear controller $K(s)$ for the linear system $G(s)$.

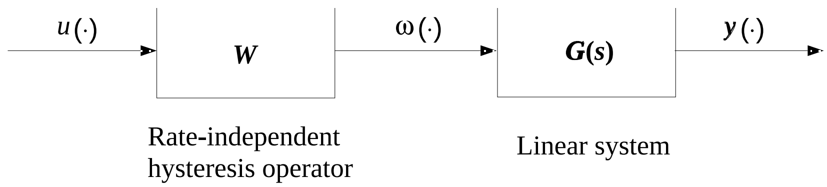

Figure 4.
Structure of models for smart actuators

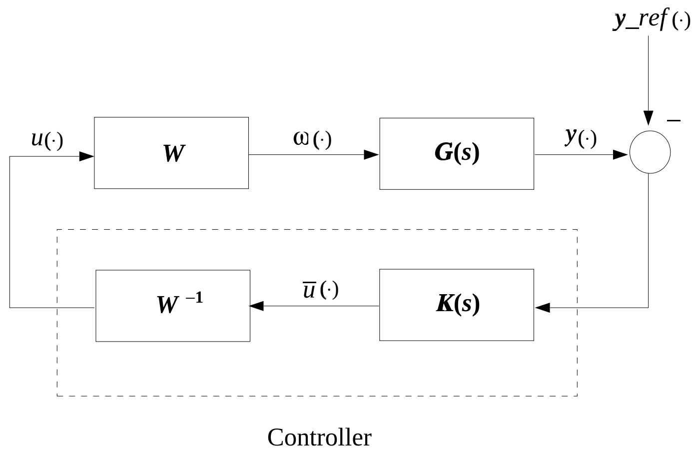

Figure 5.
Controller design schematic

In the context of this paper, we consider W as a Preisach operator. The Preisach operator is highly nonlinear, and in general, we cannot find closed form formulas for the inverse operator, unless the measure function is of some special form.[14] Hughes and Wen[6] utilized the first order reversal curves $f(\beta, \alpha)$ in computing the numerical inverse of the Preisach operator. They define $F(\beta, \alpha) = \frac{1}{2}[f(\alpha, \alpha) - f(\beta, \alpha)]$(called the *Everett surface).*For output change $\triangle\omega$,

$$\triangle\omega = 2F(\beta, \alpha) \tag{7}$$

defines two inverse maps $G_\alpha(\cdot, \cdot)$ and $G_\beta(\cdot, \cdot)$:

$$\alpha = G_\alpha(\triangle\omega, \beta), \tag{8}$$
$$\beta = G_\beta(\beta, \triangle\omega). \tag{9}$$

$G_\alpha(\cdot, \cdot)$ and $G_\beta(\cdot, \cdot)$ is then used to compute the desired input given the desired output and past input history. This method relies on measurement of all first order reversal curves and therefore is subject to experimental errors. Also computing G_α, G_β involves solving nonlinear equations and therefore is not a trivial task.

4.1. Contraction mapping algorithm for inversion

Under mild assumptions, the Preisach operator is Lipshitz continuous and incrementally strictly increasing.[10] Venkataraman and Krishnaprasad[15,16] exploited these properties and proposed an inversion algorithm for the Preisach operator based on the contraction mapping principle. The algorithm is summarized in the following theorem:

Theorem 4.1:[Contraction Mapping Algorithm for Inversion][15,16] *Let* $X = C_I[0, T]$*, where*$I = [a, b]$*.* $C_I[0, T]$ *denotes the space of continous functions defined on* $[0, T]$ *taking values in* I*. Let* $\Gamma : X \to Y$*, where* Γ *is a* *strictly increasing, strongly Lipshitz continuous Preisach operator (with Lipshitz constant k_2), some initial memory curve ψ_{-1}, and Y is the range of Γ. Let $\epsilon > 0$ and the operator equation*

$$\Gamma(x) = y, \tag{10}$$

where $y \in Y$ is given. Consider the algorithm:

- *pick any $x_0 \in X$;*
- *while $\| x_n - x_{n-1} \| \geq \epsilon$:*

$$x_{n+1} = \frac{1}{k_2}(y + (k_2 x_n - \Gamma(x_n))). \tag{11}$$

The sequence $\{x_n\}$ terminates at z which satisfies $\| z - x \| \leq \epsilon$ where x is the solution of (10). The rate of convergence is linear.

When the Preisach measure is discretized, the Preisach operator is no longer Lipschitz continuous and therefore the contraction mapping algorithm for inversion does not work efficiently. Indeed, since the output of Γ at any time instant can take only finite number of possible values (due to the finite number of measure atoms), from (11), we see that for almost all y,

$$\| x_n - x_{n-1} \| = \frac{1}{k_2} \| y - \Gamma(x_{n-1}) \| \geq \delta_y > 0.$$

In addition, the disrete measures are, in general, not uniform. These factors make it difficult to choose an appropriate stopping criterion ϵ: picking ϵ big we lose accuracy; picking ϵ small we will get stuck if $\epsilon < \delta_y$. Note that these remarks don't invalidate Theorem 4.1: Theorem 4.1 works perfectly for continuous measure distribution. However, we need a more practical inversion algorithm for the discrete measure case.

4.2. Closest matching algorithm for inversion

We propose a new inversion algorithm in this subsection. This algorithm, like the contraction mapping algorithm, is also based on the strictly increasing property of the Preisach operator. It fully utilizes the discrete structure of the problem. We name it *closest matching algorithm* because it always generates input whose output matches the desired output most closely among all possible inputs. We now describe the algorithm in detail.

Note that due to discretization, the input can only take values from a finite set $U \triangleq \{u_l, 1 \leq l \leq L\}$ with each $u_l, 1 \leq l \leq L$, representing an input level. To be precise, let

$$\triangle u = \frac{u_{max} - u_{min}}{L},$$

then $u_l = u_{min} + (l-1) \triangle u$. The inversion problem is: given an initial memory curve $\psi^{(0)}$(from which the initial input $u^{(0)}$ and output $\omega^{(0)}$ can be derived) and a desired output $\bar{\omega}$, find $u^* \in U$, such that

$$|\Gamma(u^*; \psi^{(0)}) - \bar{\omega}| = \min_{u \in U} |\Gamma(u; \psi^{(0)}) - \bar{\omega}|. \tag{12}$$

Also the algorithm should return the resulting memory curve ψ^*. Note in (12) we explictly put $\psi^{(0)}$ as argument of Γ to emphasize the effect of the memory curve on the output.

Closest Matching Algorithm:

- Step 0. Set n=0. Compare $\omega^{(0)}$ and $\bar{\omega}$: if $\omega^{(0)} = \bar{\omega}$, let $u^* = u^{(0)}, \psi^* = \psi^{(0)}$, go to Step 3; if $\omega^{(0)} < \bar{\omega}$, go to Step 1.1; otherwise go to Step 2.1;
- Step 1.
  - Step 1.1: If $u^n = u_L$, let $u^* = u^n, \psi^* = \psi^n$, go to Step 3; otherwise $u^{(n+1)} = u^{(n)} + \triangle u, \tilde{\psi} = \psi^{(n)}$[backup the memory curve], $n = n+1$, go to Step 1.2;

– Step 1.2: Evaluate $\omega^{(n)} = \Gamma(u^n; \psi^{(n-1)})$, and (at the same time) update the memory curve to $\psi^{(n)}$. Compare ω^n with $\bar{\omega}$: if $\omega^{(n)} = \bar{\omega}$, let $u^* = u^{(n)}, \psi^* = \psi^{(n)}$, go to Step 3; if $\omega^{(n)} < \bar{\omega}$, go to Step 1.1; otherwise go to Step 1.3;
– Step 1.3: If $|\omega^{(n)} - \bar{\omega}| \le |\omega^{(n-1)} - \bar{\omega}|$, let $u^* = u^{(n)}, \psi^* = \psi^{(n)}$, go to Step 3; otherwise $u^* = u^{(n-1)}, \psi^* = \tilde{\psi}$ [restore the memory curve], go to Step 3;

- Step 2.
  – Step 2.1: If $u^n = u_1$, let $u^* = u^n, \psi^* = \psi^n$, go to Step 3; otherwise $u^{(n+1)} = u^{(n)} - \triangle u, \tilde{\psi} = \psi^{(n)}$[backup the memory curve],$n = n + 1$, go to Step 1.2;
  – Step 2.2: Evaluate $\omega^{(n)} = \Gamma(u^n; \psi^{(n-1)})$, and (at the same time) update the memory curve to $\psi^{(n)}$. Compare ω^n with $\bar{\omega}$: if $\omega^{(n)} = \bar{\omega}$, let $u^* = u^{(n)}, \psi^* = \psi^{(n)}$, go to Step 3; if $\omega^{(n)} > \bar{\omega}$, go to Step 2.1; otherwise go to Step 2.3;
  – Step 2.3: If $|\omega^{(n)} - \bar{\omega}| \le |\omega^{(n-1)} - \bar{\omega}|$, let $u^* = u^{(n)}, \psi^* = \psi^{(n)}$, go to Step 3; otherwise $u^* = u^{(n-1)}, \psi^* = \tilde{\psi}$ [restore the memory curve], go to Step 3;
- Step 3. Exit.

It's not hard to see the above algorithm yields the best input u^* in at most L iterations.

5. EXPERIMENTAL RESULTS

In this section, we will apply the identification and inversion schemes to open loop control of a magnetostrictive actuator. Magnetostriction is the phenomenon of strong coupling between magnetic properties and mechanical properties of some ferromagnetic materials (e.g., Terfenol-D): strains are generated in response to an applied magnetic field, while conversely, mechanical stresses in the materials produce measurable changes in magnetization. Figure 6 shows a sectional view of a Terfenol-D actuator manufactured by ETREMA Products, Inc. By varying the current in the coil, we vary the magnetic field in the Terfenol-D rod and thus control the motion of the rod head.

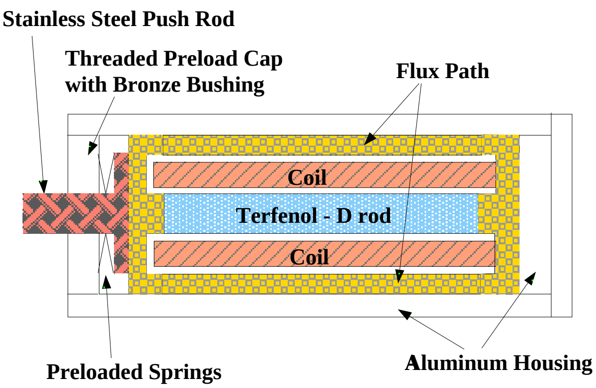

Figure 6.
Sectional view of the Terfenol-D actuator

Magnetostriction λ can be empirically expressed in terms of bulk magnetization M as[9]:

$$\lambda = \sum_{i=0}^{\infty} a_i M^{2i}. \tag{13}$$

We can obtain a reasonable approximation by including terms up to $i = 1$ and ignoring the constant term, which is simply the elastic strain and does not play an active rold in the magnetomechanical effect.[9] This gives

$$\lambda = a_1 M^2. \tag{14}$$

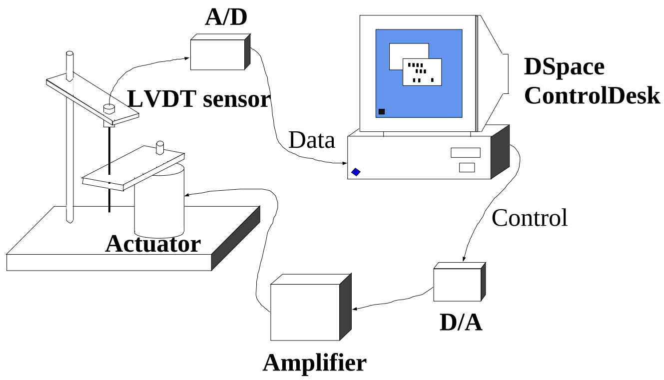

Figure 7. Experiment setup

We can identify the coefficient a_1 from the saturation magnetization M_s and the saturation magnetostriction λ_s provided by the manufacturer:

$$a_1 = \frac{\lambda_s}{M_s^2}.$$

Let the length of the magnetostrictive rod be l_{rod}. Given a measurement of the displacement d, the underlying magnetization M is determined by,

$$M = \pm\sqrt{\frac{d}{a_1 l_{rod}}}, \tag{15}$$

and the sign of M is determined with further information on the input. The applied magnetic field H is related to the input current through

$$H = NI + H_{bias}, \tag{16}$$

where N is the number of coils per unit length and H_{bias} is the bias magnetic field produced by permanent magnets. H_{bias} is necessary for generating bidirectional strains and it can be identified easily.

We will treat the magnetic field H as input and the bulk magnetization M as output using transformations (15) and (16). And we employ the Preisach operator to model the hysteretic relationship between M and H. We will identify the Preisach measure, and then carry out inverse compensation based on the identified measure. An open loop tracking experiment will be done to check the performance of the identification and inversion algorithms.

5.1. Experiment setup

Our experimental setup is as shown in Figure 7. DSpace ControlDesk is a powerful tool for real-time simulation and control. It can generate system models from Simulink of Matlab, downloads real-time applications into a DSP board, and collect data or send out commands to monitor and control a system in real time. The data it collects can be displayed or be saved on disk for post-processing. The displacement of the actuator is measured with a LVDT sensor.

5.2. Measure identification and validation

The magnetic field input H is limited in the range [-40 Oe, 480 Oe] and is discretized into 26 levels. Figure 8 shows distribution of the identified measures. The constant contribution from Ω_0 (see Figure 3) is estimated to be 0.3466.

To verify the identified measures, we apply same input signal (which differs from the input used for identification) to the actuator and the Preisach model. Figure 9 shows the comparison of the actuator output and the output of the Preisach model. We can see they agree reasonably well and therefore the identified Preisach operator provides a good approximation to the actuator.

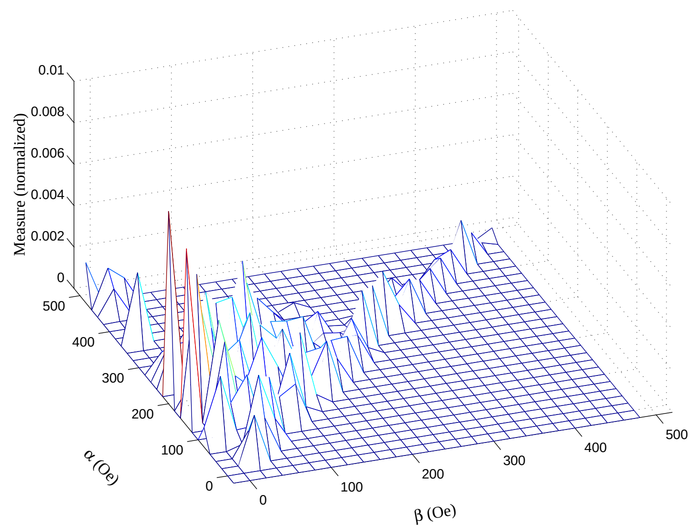

Figure 8. Distribution of identified measures

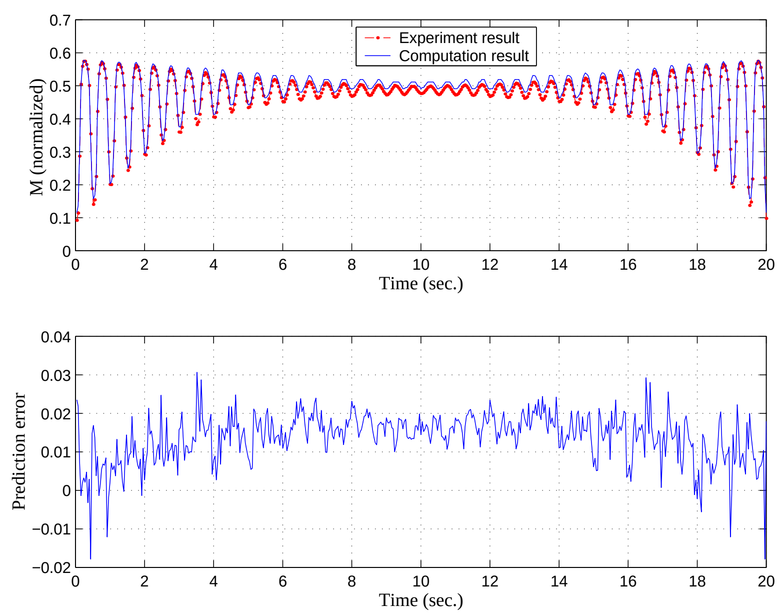

Figure 9. Validation of identified measures

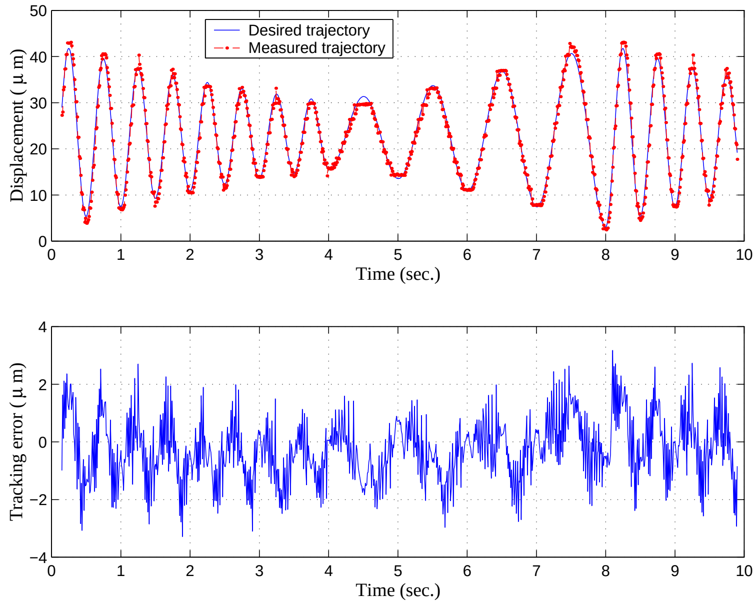

Figure 10. Distribution of identified measures

5.3. Open loop tracking experiment

Finally, we do an open loop tracking experiment to test the overall performance of our identificaiton and inversion scheme. Given a desired trajectory, whose amplitude and frequency are both varying, we compute a desired input using the closest matching inversion algorithm. The computed input signal is then sent to the actuator and the displacement trajectory is measured. Figure 10 shows the comparison of the desired trajectory and the actual trajectory. The tracking error lies within a small interval $[-3\mu m, 3\mu m]$.

6. CONCLUSIONS AND FUTURE WORK

In this paper, we have proposed a systematic approach for control of smart actuators. We model the hysteresis by the Preisach operator and identify the Preisach measure using a constrained least square method. We have presented an inversion algorithm based on the strictly increasing property of the Preisach operator. The effectiveness of our approach is demonstrated via an open-loop trajectory tracking experiment.

There are a couple of possible and interesting directions to extend this work:

- The current inversion algorithm generates input in a discrete value set and thus it is not continuous. This drawback can be taken care of by interpolation between the computed values.
- We have identified measures for *discrete atoms* in the Preisach plane. Sometimes a continuous measure function is more useful, especially if we want to do some analysis on the system. In that case, we may fit a smooth surface from the identified discrete measure masses.
- It is well known that properties of smart actuators may vary with time, temperature, etc. This means we might need to re-identify the model quite often or even on-line identification is necessary. Also Off-the-shelf algorithms for solving the constrained least squares problem can be very time-consuming when the discretization gets fine. Therefore a fast and efficient algorithm will be very useful.

REFERENCES

1. G. Tao and P. Kokotović, "Adaptive control of plants with unkown hystereses," *IEEE. Trans. Automat. Contr.* **40**(2), pp. 200–212, 1995.

2. R. Smith, "Inverse compensation for hysteresis magnetostrictive transducers," *CRSC Technical Report CRSC-TR98-36* , 1998.
3. W. Galinaitis and R. Rogers, "Control of a hysteretic actuator using inverse hysteresis compensation," in *Mathematics and Control in Smart Structures*, V. Varadhan, ed., *Proc. SPIE* **3323**, pp. 267–277, 1998.
4. D. Jiles and D. Atherton, "Theory of ferromagnetic hysteresis," *J. Magn. Magn. Mater.* **61**, pp. 48–60, 1986.
5. A. Adly, I. Mayeygoyz, and A. Bergqvist, "Preisach modeling of magnetostrictive hysteresis," *J. Appl. Phys.* **69**(8), pp. 5777–5779, 1991.
6. D. Hughes and J. Wen, "Preisach modeling and compensation for smart material hysteresis," in *Active Materials and Smart Structures*, *Proc. SPIE* **2427**, pp. 50–64, 1994.
7. R. Gorbet, D. Wang, and K. Morris, "Preisach model identification of a two-wire SMA actuator," in *Proceedings of IEEE International Conference on Robotics and Automation*, pp. 2161–2167, 1998.
8. I. Mayergoyz, *Mathematical Models of Hysteresis*, Springer Verlag, New York, 1991.
9. D. Jiles, "Theory of the magnetomechanical effect," *Phys. D: Appl. Phys.* **28**, pp. 1537–1546, 1995.
10. M. Brokate and J. Sprekels, *Hysteresis and Phase Transitions*, Springer Verlag, New York, 1996.
11. K.-H. Hoffmann and J. Sprekels, "Identification of hysteresis loops," *J. Comput. Phys.* **78**, pp. 215–230, 1988.
12. K.-H. Hoffmann and G. Meyer, "A least squares method for finding the Preisach hysteresis operator from measurements," *Numer. Math.* **55**, pp. 695–710, 1989.
13. R. Venkataraman, *Modeling and Adaptive Control of Magnetostrictive Actuators*, Ph. D. thesis, University of Maryland, College Park, available at: $http://www.isr.umd.edu/TechReports/ISR/1999/PhD\_99-1/PhD\_99-1.phtml$, 1999.
14. W. Galinaitis and R. Rogers, "Compensation for hysteresis using bivariate Preisach models," in *Mathematics and Control in Smart Structures*, V. Varadhan and J. Chandra, eds., *Proc. SPIE* **3039**, pp. 538–547, 1997.
15. R. Venkataraman and P. Krishnaprasad, "A novel algorithm for the inversion of the Preisach operator," in *Mathematics and Control in Smart Structures*, V. Varadhan, ed., *Proc. SPIE* **3984**, pp. 404–414, 2000.
16. R. Venkataraman and P. Krishnaprasad, "Approximate inversion of hysteresis: theory and numerical results," in *Proceedings of the 39th IEEE Conference on Decision and Control*, pp. 4448–4454, 2000.